Rev. Roum. Sci. Techn.– Électrotechn. et Énerg.
Vol. **71**, *4*, pp. 567–572, Bucarest, 2026

EXPERIMENTAL INVESTIGATION OF MELTING PROCESS

DIHIA DJEFEL [1], SAID MAKHLOUF[1]

Keywords: Heat energy storage; Heat exchanger; Phase change materials; Melting process.

This paper presents an experimental study of the melting characteristics of a PCM rectangular thermal storage system. The LHESS is composed of a shell and tubes with circulating heat transfer fluid (HTF; water in this study). Stearic acid is used as the PCM and placed in the space between the shell and tubes. The melting process of the phase change material is investigated with flow rate and inlet temperature parameters. According to the experimental results, as the inlet temperature was increased by 65°C, 75°C, and 80°C, the melting time was 51%, 64.46%, and 73.28%, respectively, for a fluid flow rate of 4.61 l/min. Moreover, the results showed that the effect of HTF flow on the thermal energy storage (TES) is 9%, 10%, and 15% for the flow rates of 4.61 l/min, 4.61 l/min, and 1 l. / min, respectively.

1. INTRODUCTION

The increasing integration of renewable energy sources and the need to improve energy efficiency have made thermal energy storage (TES) an essential technology for balancing energy supply and demand. Among the available TES technologies, latent heat thermal energy storage (LHTES) based on phase change materials (PCMs) has attracted considerable attention because of its high energy storage density, nearly isothermal operation during phase transition, and suitability for low- and medium-temperature applications [1–4].

Despite these advantages, the low thermal conductivity of most PCMs remains the main limitation to their practical application, leading to long charging and discharging times. As a result, extensive research has been devoted to enhancing heat transfer performance through optimized heat exchanger configurations, extended surfaces (fins), high-conductivity additives, and improved operating strategies [5–8].

Shell-and-tube latent heat storage systems have been widely investigated both experimentally and numerically. It is well established that the melting and solidification processes are strongly influenced by the *Heat Transfer Fluid* (HTF) operating conditions. Increasing the HTF inlet temperature enhances the temperature gradient between the fluid and the PCM, thereby accelerating the melting process, while higher mass flow rates improve the convective heat transfer coefficient and reduce charging time [9–12]. In addition, the use of fins, metal matrices, or composite PCMs has been shown to significantly reduce thermal resistance and improve energy storage performance [6,8,13].

Although these studies have significantly improved the understanding of heat transfer mechanisms in LHTES systems, most of the available literature has focused on paraffin-based PCMs such as RT35, RT50, or paraffin wax. Comparatively fewer studies have addressed fatty-acid PCMs under realistic operating conditions. Moreover, existing works generally report the influence of individual parameters (temperature or flow rate) on charging time without establishing combined relationships that could support the design and optimization of storage systems. Consequently, the coupled effects of HTF inlet temperature and mass flow rate on the performance of shell-and-tube systems using stearic acid remain insufficiently documented.

Stearic acid is a promising PCM for low-temperature thermal energy storage due to its relatively high latent heat of fusion, good thermal and chemical stability, low supercooling tendency, and excellent cycling reliability. In addition, fatty acids such as stearic acid offer advantages over paraffins in terms of non-toxicity, biodegradability, and stable thermophysical properties, making them suitable for domestic solar thermal systems and waste heat recovery applications [4,14,15]. However, despite these advantages, experimental data on stearic acid in shell-and-tube latent heat storage systems remain limited compared to conventional paraffin-based materials.

The present work aims to experimentally investigate the charging behavior of a shell-and-tube latent heat thermal energy storage unit using stearic acid as the PCM. The effects of HTF inlet temperature and mass flow rate on the melting process are systematically analyzed in terms of temperature evolution, melting front progression, and charging time. Beyond confirming the influence of these operating parameters, the study provides a comparative analysis of their relative impact on system performance, with the objective of contributing to the development of design guidelines for stearic-acid-based latent heat storage systems. The experimental results also provide valuable reference data for the validation of numerical models and the design of future PCM-based thermal energy storage units.

2. MATERIALS AND METHODS

2.1 EXPERIMENTAL SETUP

Figure 1 illustrates the schematic diagram and photograph of the system created in this study. Stearic acid, which has a melting range of approximately 50-56°C, was used as PCM for energy storage. When the PCM melts, thermal energy is stored. In Fig. 1, the heat transfer fluid (HTF) passed through a flowmeter by means of a pump, and the mass flow rate of the fluid was fixed at the desired level. The HTF, heated by the hot water in a water bath, passed through the admission collector and then the aluminum U-tube heat exchanger, reaching the test area (charge). As the hot water flowed through the U-tubes in the test area, the PCM (SA), located between the outer surface of the tubes and the inner surface of the plexiglass, melted (charge). Temperature values that changed in the test area were taken with the help of a data logger. The recorded measurement data showed the instantaneous temperature values of the thermocouples in the test area. Its working principle is based on converting a voltage, generated by the temperature difference between the junctions, into a temperature value. Pico Technology Data Logger was used. In this study, the TES performance of the PCM, located between the outer surface of the U-tube heat

[1,2] Dept. of Mechanics, LMSE Laboratory, Faculty of Construction Engineering, Mouloud Mammeri University of Tizi Ouzou, BP 17, RP 15000, Tizi Ouzou, Algeria.
Emails: dihia.djefel@ummto.dz, said.makhlouf@ummto.dz

DOI: 10.59277/RRST-EE.2026.4.15

exchanger through which the HTF passes and the inner surface of the plexiglass enclosure, was experimentally investigated by varying HTF parameters.

2.1.1 INSTRUMENTATION OF THE TEST SECTION

The PCM storage unit considered in this work is a rectangular transparent Plexiglas box, with dimensions 70 x 200 x 85 mm³ and a thickness of 10 mm, to allow the observation of the fusion process. The exchanger of a car radiator is used to circulate the heat transfer fluid. This exchanger is made up of 8 U-shaped tubes whose tube inlets are connected to a distributor, while the tube outlets are connected to a collector. The exchanger used consists of eight U-shaped tubes with a height of 0.5 m and exterior and interior radii of 8.4 mm and 8 mm, respectively. A void is left in the upper part of the case to allow expansion of the PCM volume.

The locations of the inserted thermocouples are indicated in Fig. 2 and Table 1. The measurement setup incorporates K-type thermocouples, enabling the monitoring of temperature variations within the measurement circuit. Specifically, two thermocouple probes, positioned at the water inlet and outlet, are inserted at the entry and exit points of the water within the circulation pipe. Additionally, six other thermocouples (T1 to T6) are strategically placed inside the container. All measurements from the various thermocouples are retrieved and recorded by a PicoLog data logger and a laptop PC.

The positions where thermocouples are situated are provided in Table 1.

Table 1

Axial positions of the thermocouples.

Thermocouple	Height (mm)	Length (mm)	Width (mm)
T1	259.98	100	1
T2	216.65	100	1
T3	173.32	100	1
T4	129.99	100	1
T5	86.66	100	1
T6	43.33	100	1

2.1.2 SELECTION AND PROPERTIES OF PCM

In this investigation, a commercially available Stearic Acid (SA), specifically referenced as S4751 and manufactured by Sigma-Aldrich, serves as the latent heat energy storage material. SA is characterized as a linear-chain N-alkane with the chemical formula CH3(CH2)16COOH. It functions as a solid-liquid phase change material (PCM) with a latent heat capacity of 190 KJ/kg. Notably, SA exhibits minimal subcooling, chemical stability, non-corrosiveness with most packaging materials, and is economically viable. Table 2 provides an overview of the thermophysical properties of SA.

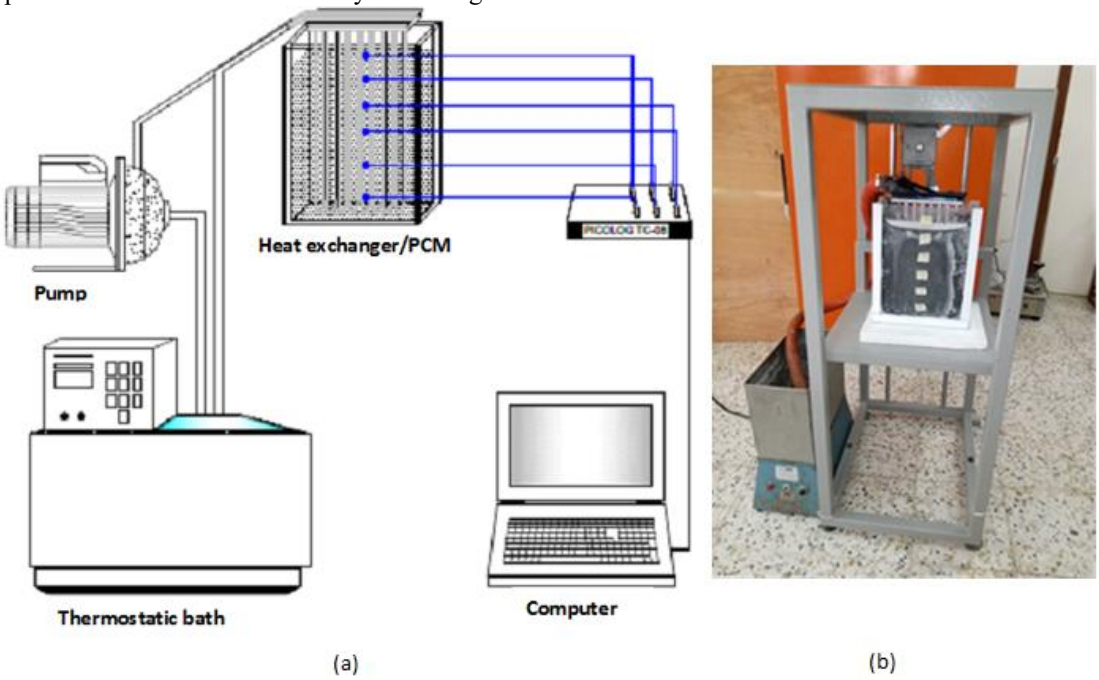


Fig. 1 – Symmetry, Illustration of the a) experimental setup circuit in schematic form, accompanied by its b) photograph.

Table 3

DSC analysis results.

Sample	five-cycle average of DSC analysis							
	Thermal poperties of solidification process				Thermal poperties of melting process			
	T_{ss} (°C)	T_{Ps} (°C) Pic	T_{es} (°C)	Latent heat (J.g $^{-1}$)	T_{sf} (°C)	T_{PF} (°C) Pic	T_{eF} (°C)	Latent heat (J.g^{-1})
AS-1	52.78	52.03	50.53	189.54	53.33	55.26	56.19	186.37
AS-5	52.32	51.2	47.47	190.17	52.81	55.77	58.7	196.39
AS-10	51.70	48.53	44.09	191.39	52.67	57.32	61.83	188.4

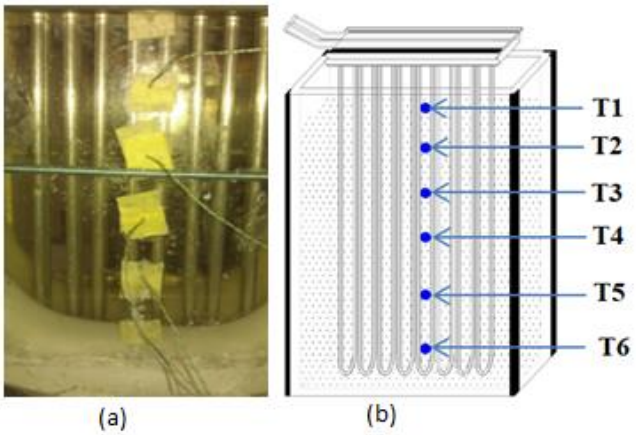


Fig. 2 – Picture of a) the test section; b) Schematic representation of the vertical division. The gray cylinder represents the U-shaped tubes. The PMMA box is shown in solid black lines. Instrumentation: The blue dots correspond to type K thermocouples.

Differential scanning calorimetry (DSC) is a thermal analysis method that measures changes in temperature and heat over time and temperature in a controlled environment. This technique provides both qualitative and quantitative information on physical and chemical transformations, particularly those associated with endothermic or exothermic processes. DSC analysis is used to characterize the identity of the phase change material (PCM). Figure 3 and Table 3 illustrate the thermophysical properties of SA-PCM determined by DSC analysis.

2.2 EXPERIMENTAL ERROR ANALYSIS

Uncertainty analysis must be considered to verify the accuracy of the experimental data that has been collected. The precision of the collected experimental data depends on the devices and measuring instruments. Calibrated thermocouples, flowmeters, and thermostatic baths were used. The uncertainty analysis of the measuring instruments used is presented in Table 4.

Table 2

Axial and radial positions of the thermocouples.

Properties	Stearic Acid
M (kg/kmol)	284.483*
d_s at 25 °C (kg/m^3)	0.9408
d_l at 60 °C (kg/m^3)	0.2844*
T (°C):	
Tm	56
Ts	50.42
L (kJ/kg.K):	
Lm	190.47
Ls	189.36
Cp (J/kg.K):	
Cps at 26°C	1250.1
Cpl at 69°C	2300
K (W/m.K)	
Ks	0.2
Kl	0.172*
μ à 72 °C (Pa·s)	0.009*
β at 69 °C (°C-1)	0.00029

*Calculated with reference [15]

The analysis of the error by calculating the flow rate parameter of the water circulating in the exchanger, using McClintock and Kline (1953), is 3.97%.

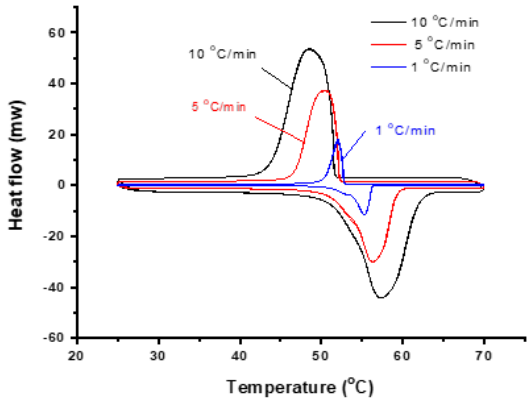


Fig. 3 – Differential scanning calorimetry analysis curve of the SA-PCM.

Table 4

Uncertainty of measuring device parameters.

Measuring device	Device model	Uncertainty	Device range
Thermocouple	K type	(±0.025)	-270 to +1820
Flow meter	LZM-15G	(±0.1)	0-12 l/min
thermostatic bath	B052-01-30l	(±1°C)	0-100

3. RESULTS

Several experiments were conducted to verify the repeatability of the results. The repeatability of the experiment for the PCM alone was carried out with an HTF inlet temperature of 75°C using a water flow rate of 4.61 l/min (experimentally determined to achieve lower uncertainty in energy calculations for higher flow rates). The experiments produced repeatable results, as can be seen in Fig. 4, which shows the temperature profiles of the PCM for three loading process operations.

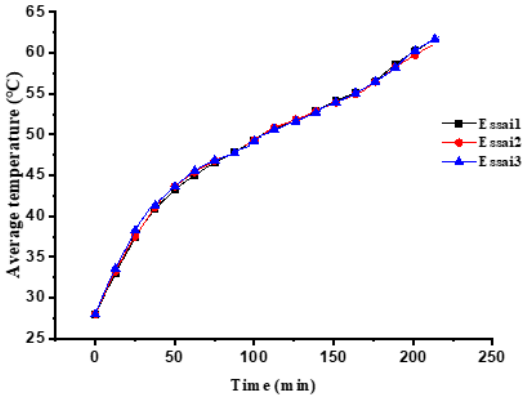


Fig. 4 – Average temperature profiles as a function of time during the loading process for three identical experiments (flow rate: 4.61 l/min).

The average temperatures of the PCM measured by the probes reached stable values after approximately 260 minutes of loading. This indicates that the melting of the PCM is complete. Figure 4 shows the same temperature profiles in each of the three loading experiments, thus demonstrating the repeatability of the experiment. The inlet temperature of the heat transfer fluid of 75 ± 0.5°C represents the average value over the experiment. This inlet temperature is subject to fluctuations due to the thermostat's activation on the resistance of the bath used.

The thermal behavior in the charging process of the TES

[1,2] Dept. of Mechanics, LMSE Laboratory, Faculty of Construction Engineering, Mouloud Mammeri University of Tizi Ouzou, BP 17, RP 15000, Tizi Ouzou, Algeria.
Emails: dihia.djefel@ummto.dz, said.makhlouf@ummto.dz

DOI: 10.59277/RRST-EE.2026.4.15

system is studied under different operating conditions in the following sections. A series of tests was conducted to explore the mechanisms of melting. The temperature profiles inside the container that determine the dominant mode of heat transfer during different stages of phase change are presented. The effects of variations in two primary experimental parameters, HTF inlet temperature and HTF flow, are investigated. Temperature profiles of thermocouples at different HTF inlet temperatures and HTF flow rates are presented in this section to provide an understanding of the heat transfer mechanism within stearic acid during the loading phase.

3.1 IMPACT OF HTF FLOW RATE

Figures 5 to 7 represent temperature profiles obtained with thermocouple probes from T2 to T6 with an HTF inlet temperature of 75 °C at three different flow rates. Figure 5 shows the temperature variations in thermocouple probes located 1 mm from the inner surface of the acrylic rectangle in the vessel under an HTF inlet temperature of 75 °C and a flow rate of 1 L/min. It is seen that the PCM temperatures at different height levels reach the melting temperature at different times. The time it takes for PCM to melt at higher levels is shorter than at lower levels. This is due to the natural convection that occurs in the liquid part of the molten PCM, as indicated in the literature [10,12]. It should be noted that the mass of PCM in the first case was not completely melted. This result is confirmed by the temperature profile obtained with the thermocouple T6. It is clearly seen that the temperature does not exceed 25°C, a value very far from the temperature of the PCM in the liquid state.

On the other hand, in Fig. 5 and 6, we notice that the temperatures recorded by the thermocouples T2 to T6 reach the melting temperature of the PCM. Once the T6 thermocouple has reached a stable temperature above the melting temperature of the PCM, the total charge time is set during the charging process. Comparison of the total charge time for different throughputs in the storage system shows that increasing the throughput of the HTF reduces the charging time required for full PCM fusion for the storage system.

In the initial melting step, where the conduction heat transfer mode is dominant, the effect of HTF flow rate on the local heat transfer rate is much less pronounced than during the subsequent convection-dominated stage. Subsequently, natural convection begins to increase with the increase in HTF flow in the pipes at a faster melting rate. Because the dominant thermal resistance to heat transfer lies on the PCM side, owing to its low thermal conductivity, this resistance decreases locally as the PCM layer adjacent to the tube surface melts and starts to mix convectively. PCM near the heat transfer surfaces melts more rapidly, resulting in a rapid onset of natural convection that increases the melting rate in the PCM. A melting time of 174 minutes is recorded for thermocouple T6 at a flow rate of 4.61 l/min, whereas thermocouple T6, at a flow rate of 2.26, reaches melting in 208 minutes; at a flow rate of 1 l/min, thermocouple T6 does not reach melting within the test duration, while thermocouple T5, at a different position, reaches melting in 287 minutes.

The total time required for the full melt varies depending on the HTF rate used. For a flow rate of 4.61 l/min, the full charge time of the PCM is 236 min. It takes another hour to reach full melting for a flow rate of 2.26 l/min. The complete melting time for a flow rate of 1 l/min is longer compared to the other two previous flow rates and is 350 min.

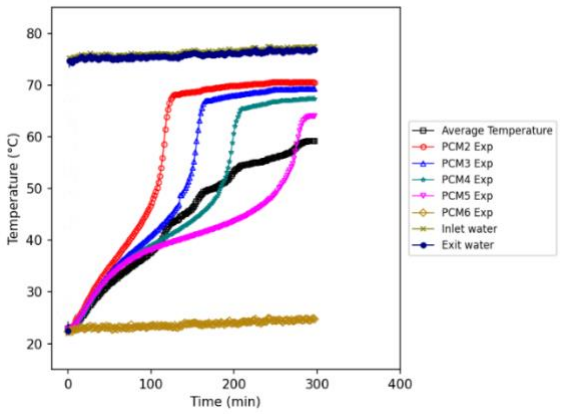


Fig. 5 – Temperature profiles from T2 to T6 with an inlet temperature of 75 °C and an HTF flow rate of 1 l/min.

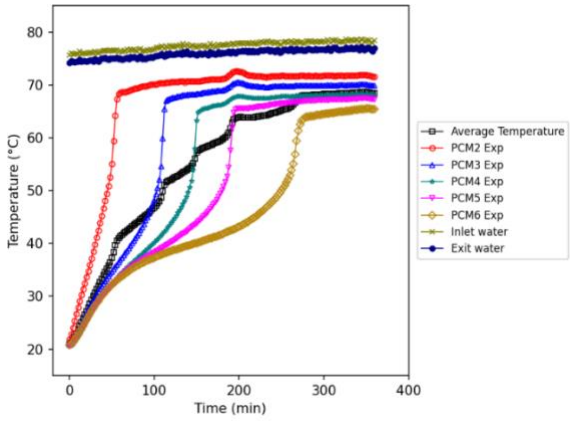


Fig. 6 – Profiles from T2 to T6 with an inlet temperature of 75 °C and a flow rate of 2.26 l/min.

3.2 IMPACT OF HTF INLET TEMPERATURE

Figure 8 shows the PCM temperature variations in the charging process for thermocouple probes located 1 mm from the inner surface of the acrylic shell in the storage system. The charging process continued until the PCM temperature in all thermocouples did not change significantly. Three different HTF loading temperatures of 65°C, 75°C, and 80°C were considered with the same HTF flow rate maintained at 4.61 L/min.

It is observed that the overall charging time strongly depends on the inlet temperature of the HTF.

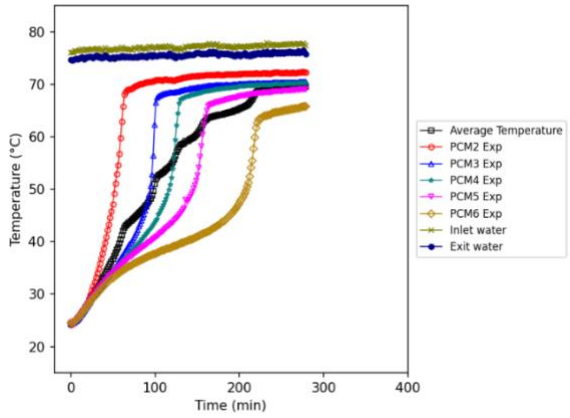


Fig. 7 – Temperature profiles from T2 to T6 at an inlet temperature of 75 °C and a flow rate of 4.61 l/min.

In addition, it has also been found that the average stable temperatures of the PCM recorded are lower than the inlet

temperatures of the HTF during the charging process. This is mainly for two reasons. First, when all the PCM has melted, the effect of natural convection decreases, and hence the heat transfer between the HTF fluid and the liquid PCM decreases. This reduces energy transfer into the PCM. Second, the inevitable heat loss from the system to the surroundings, which prevents the PCM temperature from rising.

The time required for T2 to reach the melting point for the HTF inlet temperatures of 65 °C and 80 °C is, respectively, more than 487 min (not complete fusion) and 72 min. T3 requires additional time to reach the melting temperature. The total time required for complete melting varies according to the HTF inlet temperature. The melting time as a function of the HTF inlet temperature at the same flow rate is shown in Fig. 8.

It is found that at the same distance from the pipes where the HTF circulates, faster melting and a higher temperature are obtained in the upper part. This is consistent with buoyancy-driven natural convection: as the PCM melts, the lighter liquid phase rises toward the top of the exchanger, carrying warmer fluid upward and accounting for the faster melting and higher temperatures recorded there.

Therefore, the increase in HTF inlet temperature reduces the full charge time and reaches a higher temperature in the upper part. More heat is transferred to the PCM section per unit of time. The increase in heat transfer caused by the greater temperature difference promotes faster melting at the start of the charge. This results in more liquid PCM at the top of the container, which in turn leads to a faster onset of natural convection.

The thermal storage temperature profile curves for pure stearic acid are shown in Figure 9 for 65°C, 75°C, and 80°C. In the first stage of fusion, for each test, heat is stored as sensible heat and recorded at all points. During the thermal storage process of the pure SA, the temperatures of the upper part (T1, T2 and T3) increase much more rapidly than the temperatures recorded by the thermocouples (T4, T5 and T6) placed at the bottom of the exchanger but at the same distance from the center as the thermocouples of the upper part. This is due to heat transfer dominated by natural convection, and as fusion increases, buoyancy forces drive the liquid PCM with a lower density to move to the top of the heat exchanger. The temperature of the liquid PCM is higher than that of the unmelted portion, which causes a higher temperature at the top of the heat exchanger. On the other hand, the influence of the variation of the inlet temperature of the HTF is clearly remarkable for temperatures recorded at the same points of thermocouples. Temperatures with 80 °C as the FC inlet temperature record a low melting time and a high temperature rise rate compared to the temperatures of two other tests with HTF temperatures of 75 °C and 65 °C.

In the experiments, it is found that a small portion of stearic acid at the bottom takes a longer time to melt, which increases the full charge time of the storage unit. This is due to the natural convection effect, which transfers heat to the upper part of the exchanger, and due to the low conductivity of stearic acid. This leads to low heat available to melt the PCM at the bottom of the container.

The difference in temperature between PCM and HTF is the main factor contributing to the determination of the complete melting time. Increasing the HTF flow rate results in a higher heat transfer coefficient, which leads to a greater amount of energy transferred to the PCM. However, the FC flow rate has less impact on the total melting time compared to the temperature difference between the PCM and the HTF.

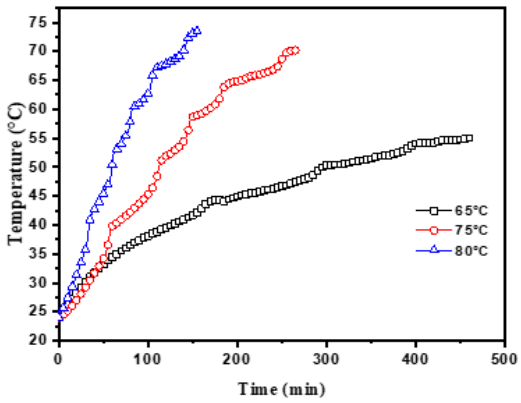


Fig. 8 – Effect of the inlet temperature on the average SA temperatures with a flow rate of 4.61 l/min.

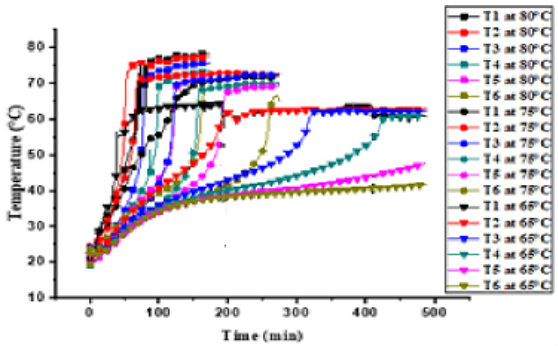


Fig. 9 – Effect of the inlet temperature on the temperatures ranging from T1 to T6 of the AS with a flow rate of 4.61 l/min.

The experimental results provide useful information beyond the charging time of the investigated prototype and can be translated into practical design recommendations for stearic acid latent heat storage systems.

The results clearly indicate that the HTF inlet temperature is the dominant operating parameter governing the charging process. Increasing the inlet temperature substantially reduces the melting time because it increases the temperature difference between the HTF and the PCM, thereby enhancing the heat transfer rate during both the conduction-dominated and convection-dominated stages. Consequently, whenever the heat source allows it, increasing the inlet temperature represents the most effective strategy for reducing charging time.

By comparison, increasing the HTF flow rate produces a smaller improvement in charging performance. At low flow rates, increasing the flow enhances the convective heat transfer coefficient inside the tubes and accelerates the melting process. However, once a sufficiently high flow rate is reached, the overall thermal resistance is mainly controlled by the low thermal conductivity of stearic acid rather than by the HTF side. Under these conditions, further increases in flow rate provide only limited reductions in charging time while increasing pumping power requirements.

The experiments also demonstrate that natural convection governs the melting process after the initial conduction stage. The upper part of the storage unit melts considerably faster than the lower part because buoyancy forces transport the warmer liquid PCM upward. This behavior suggests that

future designs should primarily focus on improving heat transfer in the lower region of the storage unit, for example by introducing fins, increasing the heat transfer surface, optimizing tube arrangement, or enhancing the thermal conductivity of the PCM.

Based on the present experimental investigation, the following practical design recommendations can be proposed for stearic acid latent heat storage systems:

- Priority should be given to increasing the HTF inlet temperature rather than excessively increasing the flow rate when rapid charging is required.
- Moderate-to-high flow rates are generally sufficient since further increases produce diminishing improvements in charging time while increasing pumping energy.
- Storage units should be designed to promote heat transfer in the lower part of the PCM where melting remains limited because of buoyancy effects.
- These observations may serve as useful design guidelines for shell-and-tube thermal energy storage systems employing stearic acid under similar operating conditions.

4. CONCLUSION

The present work experimentally investigated the charging characteristics of a shell-and-tube latent heat thermal energy storage system using commercial stearic acid as the phase change material. The effects of HTF inlet temperature and flow rate on the melting behavior and charging performance were experimentally analyzed.

Beyond confirming that both operating parameters influence the charging process, the study establishes that the HTF inlet temperature is considerably more influential than the HTF flow rate. While increasing the flow rate enhances the convective heat transfer coefficient inside the tubes, its contribution becomes progressively limited because the dominant thermal resistance shifts to the PCM side. Consequently, once moderate flow rates are achieved, increasing the HTF inlet temperature represents the most efficient approach for reducing charging time.

The experiments also demonstrate that natural convection becomes the dominant heat transfer mechanism after the initial conduction stage, producing faster melting in the upper region of the storage unit while delaying complete melting near the bottom. This observation highlights the importance of designing heat exchangers capable of improving heat transfer in the lower PCM region.

Therefore, for stearic acid-based latent heat thermal energy storage systems, the present results suggest that system optimization should primarily focus on maximizing the effective HTF inlet temperature within the allowable operating range, while selecting moderate flow rates that provide an appropriate compromise between charging performance and pumping energy consumption. These findings constitute practical design guidance that can be applied to future shell-and-tube latent heat storage systems employing stearic acid as the storage medium.

In future work, it is planned to study the horizontal TES and the maintenance of temperatures in the automobile radiator, to be able to predict the use of TES for the proper functioning of the thermal engine in the automobile.

Received on 6 February 2026

REFERENCES

1. H.K. Badaka, D.M. Kongnine, A.M. Morega, ”Heat recovery during biomass pyrolysis provided with a thermoelectric metal plate-based system,” Rev. Roum. Sci. Techn. – Électrotechn. Et Énerg., **70**, *3*, pp. 409–414 (2025).
2. F. Saftoiu, A.M. Morega, ”Cooling system for photovoltaic panels,” Rev. Roum. Sci. Techn. – Électrotechn. Et Énerg., **67**, *1*, pp. 343–348 (2022).
3. E. Douvi, et al., ”Phase change materials in solar domestic hot water systems: a review,” International Journal of Thermofluids, **10**, article 100075 (2021).
4. M. Irfan Lone, R. Jilte, ”A review on phase change materials for different applications,” Materials Today: Proceedings, **46**, pp. 10980–10986 (2021).
5. F. Agyenim, N. Hewitt, P. Eames, M. Smyth, ”A review of materials, heat transfer and phase change problem formulation for latent heat thermal energy storage systems (LHTESS),” Renewable and Sustainable Energy Reviews, **14**, *2*, pp. 615–628 (2010).
6. L. Kalapala, J.K. Devanuri, ”Influence of operational and design parameters on the performance of a PCM-based heat exchanger for thermal energy storage – a review,” Journal of Energy Storage, **20**, pp. 497–519 (2018).
7. A. Sharma, D. Buddhi, ”Effect of thermophysical properties of the PCM and heat exchanger material on the performance of a latent heat storage system,” International Journal of Solar Energy, **24**, pp. 99–105 (2005).
8. A.T. Muzhanje, H. Hassan, ”Heat transfer characteristics of charging and discharging encapsulated PCMs (SP24, SP26 & SP29) for free cooling: impact of geometry and nanomaterials addition,” J Therm Anal Calorim, **148**, *19*, pp. 9919–9936 (2023).
9. F. Agyenim, P. Eames, M. Smyth, ”Experimental study on the melting and solidification behavior of a medium temperature phase change storage material (erythritol) system augmented with fins to power a LiBr/H2O absorption cooling system,” Renew. Energy, **36**, *1*, pp. 108–117 (2011).
10. A. Hosseini, M. Rahimi, R. Bahrampoury, ”Experimental and computational evolution of a shell and tube heat exchanger as a PCM thermal storage system,” Int. Commun. Heat Mass Transf., **50**, pp. 128–136 (2014).
11. M. Rahimi, A.A. Ranjbar, D.D. Ganji, K. Sedighi, M.J. Hosseini, R. Bahrampoury, “Analysis of geometrical and operational parameters of PCM in a fin and tube heat exchanger,” International Communications in Heat and Mass Transfer, **53**, pp. 109–115 (2014).
12. A.A. Al Abidi, S. Mat, K. Sopian, M.Y. Sulaiman, C.H. Lim, ”Numerical study of melting and solidification of PCM in a triplex tube heat exchanger with and without fins,” Applied Thermal Engineering, **36**, pp. 173–182 (2012).
13. N.A. Hindi, S.F. Dakhil, K.A. Abbas, ”Experimental study to improve solar photovoltaic performance by utilizing PCM and finned wall,” Journal of Advanced Research in Fluid Mechanics and Thermal Sciences, **102**, *1*, article 1 (2023).
14. J. Jaguemont, N. Omar, P. Van den Bossche, J. Mierlo, ”Phase change materials (PCM) for automotive applications: a review,” Applied Thermal Engineering, **132**, pp. 308–320 (2018).
15. ”Yaws’ handbook of thermodynamic and physical properties of chemical compounds,” Knovel, online resource (accessed Jan. 10, 2019), https://app.knovel.com/